agronomy

MDPI

Article

RNAi-Mediated Interference with *EonuGR1* Affects the Recognition of Phenylacetaldehyde by *Empoasca onukii* Matsuda (Hemiptera: Cicadellidae)

Ruirui Zhang [1,2], Xiaoyue Lun [2], Yunhe Zhao [2], Yu Zhang [2], Yan Cao [2], Xiangzhi Zhang [2], Meina Jin [2], Zhengqun Zhang [2,*] and Xiuxiu Xu [1,*]

[1] Tea Research Institute, Shandong Academy of Agricultural Science, Jinan 250100, China; zhangruirui7275@163.com
[2] College of Horticulture Science and Engineering, Shandong Agricultural University, Tai'an 271000, China
* Correspondence: zqzhang@sdau.edu.cn (Z.Z.); yuayu88-66@163.com (X.X.)

Abstract: *Empoasca onukii* Matsuda is a primary pest of the tea plant *Camellia sinensis* (L.) O. Ktze that severely influences the production and quality of tea products. Gustatory receptors (GRs) are an indispensable part of the *E. onukii* chemosensory machinery as members of the G-protein coupled receptor family. Insect odor and gustatory receptors are consumingly sensitive and selective sensory receptors to search for foraging, mates, and spawning sites. In this study, the gustatory receptor *EonuGR1* was cloned and analyzed bioinformatically, and the expression levels of *EonuGR1* in diverse tissues of *E. onukii* were tested via qRT-PCR. The behavioral response of *E. onukii* to volatile compounds was determined via RNA interference and Y-tube olfactometer assays to investigate the role of *EonuGR1* in the olfactory recognition of *E. onukii*. The coding sequence length of *EonuGR1* was 1062 bp, and the length of the protein encoded by *EonuGR1* was 40.52 kD. The highest interference efficiency was observed after 3 h of dsEonuGR1 treatment via root soak treatment. Moreover, the response rates to phenylacetaldehyde at concentrations of 10 and 0.1 μL/mL were significantly downregulated in *E. onukii*. The responses to phenylacetaldehyde at concentrations of 10 and 100 μL/mL showed a significant decrease after dsEonuGR1 treatment for 12 h in *E. onukii*. In conclusion, *EonuGR1* was highly expressed in the abdomen and functioned in olfactory recognition of the tea plant volatile phenylacetaldehyde by *E. onukii*. Overall, *EonuGR1* has the potential as a gene target for the design of effective control strategies against *E. onukii*.

Keywords: *Empoasca onukii* Matsuda; *EonuGR1*; RNA interference; tea plant volatiles

check for updates

Citation: Zhang, R.; Lun, X.; Zhao, Y.; Zhang, Y.; Cao, Y.; Zhang, X.; Jin, M.; Zhang, Z.; Xu, X. RNAi-Mediated Interference with *EonuGR1* Affects the Recognition of Phenylacetaldehyde by *Empoasca onukii* Matsuda (Hemiptera: Cicadellidae). *Agronomy* **2023**, *13*, 2221. https://doi.org/10.3390/agronomy13092221

Academic Editors: Lanzhi Han and Fajun Chen

Received: 18 July 2023
Revised: 22 August 2023
Accepted: 24 August 2023
Published: 25 August 2023

Copyright: © 2023 by the authors. Licensee MDPI, Basel, Switzerland. This article is an open access article distributed under the terms and conditions of the Creative Commons Attribution (CC BY) license (https://creativecommons.org/licenses/by/4.0/).

1. Introduction

Tea is a common nonalcoholic beverage worldwide, and it is considered a daily necessity in many countries [1]. Tea plants are susceptible to various diseases and pests, which can depreciate tea production and economic efficiency. The tea green leafhopper, *Empoasca onukii* (Matsuda), is a serious pest of tea trees *Camellia sinensis* (L.) O. Ktze, in China [2]. In tea production, the overuse of chemical pesticides is the most widespread method to protect tea trees from *E. onukii* assaults [3]. Excessive usage of pesticides could lead to contamination of tea products and tea plantation ecosystems, ultimately posing a risk to biodiversity and human health [4]. Therefore, novel management of pest practices should be explored to help reduce the adverse costs of pest control chemicals.

Odor and gustation systems play an imperative role in the survival and reproduction of insects, such as foraging, mating selection, and spawning sites [5,6]. Olfaction is amenable to host localization, whereas gustation exercises a crucial function in host selection [7]. A crucial development in insect gustation was the classification of the gustatory receptors (GRs) family in *Drosophila melanogaster* [8,9]. Insect GRs specifically recognize gustation molecules, open ion channels, and transmit nerve impulses to higher gustation

centers, such as the suboesophageal ganglion (SOG), thus finalizing specific compound recognition, which causes insects to exhibit avoidance, detoxification, and other behavioral responses [10]. GRs pertain to the family of G-protein coupled receptors (GPCR) and have seven transmembrane domains (TMDs) [11,12]. GRs have been identified in Hemiptera, such as *Cyrtorhinus lividipennis* [13], *Riptortus pedestris* [14], *Sogatella furcifera* [15], and *Nilaparvata lugens* [16]. Numbers of GRs were highly variable across different insect species, and sequence similarity was low. Insect GRs are expressed in various insect tissues, including legs, ovipositors, and mouthparts [17]. *Helicoverpa armigera HarmGR9* was highly expressed in the foregut and abdomen [18]. *Plagiodera versicolora PverGR15* was expressed at higher levels in the antennae and forelegs [19], and tissue expressions could help in the prediction and exploration of gene functions.

Insect GRs have diverse functions in recognizing different compounds, divided into four classes based on ligand selectivity: sugar [20,21], Gr43a-like [22], CO_2 [23], and bitter receptors [24]. The model organism *D. melanogaster* has a crucial role in the functional exploration of GRs [25]. Different sugar receptors (including GR64a, GR64b, GR64c, GR61a, and GR5a) are expressed in combination with *D. melanogaster* sugar-sensitive sensors [26]. Some GRs (including Gr39a, Gr89a, Gr1a, and Gr9a) are highly sensitive to the detection of bitter substances in *D. melanogaster* [27]. Five GRs (including GR47a, GR32a, GR33a, GR66a, and GR22e) were found to participate in the identification of strychnine in *D. melanogaster* [28–30]. In *Trichogramma chilonis*, coexpression of *TchiGR64f1* and *TchiGR64f2* achieved tuning to sucrose, while expressing either alone produced no response [31]. Three CO_2 receptors (including GR1, GR2, and GR3) were identified among lepidopteran insects [12], such as *H. armigera* [32], *Mythimna separata* [33], and *Helicoverpa assulta* [34].

Expression of specific GRs could be knocked down using RNAi for gene functional studies with electrophysiological and behavioral methods [16,35]. For example, *PxutGR1* is specifically involved in synephrine recognition in *Papilio xuthus,* and the response of tarsal taste sensilla to synephrine was patently decreased when double-stranded RNA(dsRNA) was injected into insect pupae [36]. *PxylGR34* knockdown via RNAi attenuated the gustation responses to brassinolide and abolished brassinolide-induced inhibition of feeding in *Plutella xylostella* [37]. Knockdown of *PrapGR28* in *Pieris rapae* diminished the action of adult insects, medial tarsal sensilla about sinigrin [38].

An understanding of the mechanism of interaction between insect GRs and compound recognition is essential for the future development of *E. onukii* management strategies. Currently, there is a shortage of research on the function of *E. onukii* GRs. In our previous study, we identified three GRs in *E. onukii*, and found that *EonuGR1* was expressed in the antennae and body [39]. To investigate the potential contribution of GRs in the *E. onukii* antennae and body to the perception of plant volatiles, we chose *EonuGR1* as the study object. In this study, *EonuGR1* was cloned and bioinformatically analyzed, and the expression of *EonuGR1* in *E. onukii* disparate tissues was detected via qRT-PCR. The role of *EonuGR1* in recognition of compounds using olfactory was studied through a combination of RNAi and behavioral tests. In the future, GR-targeted control strategies like biochemical pesticides and insect behavior regulators for *E. onukii* could be designed based on the study of the function of *EonuGR1*.

2. Materials and Methods

2.1. Insect Culture and Reagent Materials

E. onukii adults of mixed sex and age were collected using sweep nets from tea plants in a tea garden at Taishan Chaxi Valley Agricultural Development Co., Tai'an, China, in 2022. Then, *E. onukii* were brought to the laboratory of Shandong Agricultural University (Tai'an, China) for rearing. *E. onukii* were reared on fresh 'Fudingdabai' tea branches, which were harvested from the Taishan Chaxi Valley Agricultural Development Co. and moisturized with floral foam. The tea branches were replaced every 3 days to ensure adequate food for *E. onukii*. *E. onukii* were reared in an artificial climate chamber, and our rearing conditions were 25 ± 1 °C, relative humidity of 60 ± 5%, and photoperiod of 16 h:8 h (L:D).

The volatile compounds used in our experiments were as follows: acetone (98%, Macklin, Shanghai, China), 1-phenylethanol (98%, Macklin), phenylacetaldehyde (95%, Macklin), and acetophenone (99%, Macklin).

2.2. Total RNA Isolation

Fifty adults of *E. onukii* with uniform developmental and growth states were selected for total RNA extraction. Total RNA was isolated by a FastPure® Cell/Tissue Total RNA Isolation Kit (Vazyme, Nanjing, China), and the absorbance value OD_{260nm}/OD_{280nm} of the sample RNA was measured via a microspectrophotometer (Thermo Fisher, Waltham, MA, USA). The cDNA was synthesized by reverse transcription after removal of genomic DNA using MonScriptTm RTIll All-in-One Mix (Mona, Su'zhou, China) and stored at −20 °C. The cDNA of the adult *E. onukii* was used as a template, and primers specific for *EonuGR1* were designed using Primer Premier 5.0 software, followed by PCR amplification (Table 1). All primers were synthesized by Shenggong Bioengineering (Shanghai) Co., Ltd. The 50 μL PCR system contained 1 μL of dNTP Mix (10 mM each), 25 μL of 2× Phanta Max Buffer dNTP Mix, 1 μL of Phanta Max Super-Fidelity DNA Polymerase, 2 μL each of 10 μmol/L forward and reverse primers, 1 μL of cDNA template, and 18 μL of ddH_2O. The thermal cycling conditions were 95 °C for 3 min, then 35 cycles of 95 °C for 15 s, 55 °C for 15 s, then 72 °C for 60 s, followed by incubation at 72 °C for 5 min.

Table 1. *EonuGR1* Primers used during the experiment.

Gene Name	Forward Primer	Reverse Primer	PCR Category
EonuGR1	GGGGTACCATGCCATTTGGTATTGGACAAG	CCGCTCGAGCTAAATTTGATCCATGATTCTTAAAGTTCTTG	RT-PCR
EonuGR1	TAGCAACTCAAGTAACCATCTA	CTTAACAACCTCATTATGTCCTT	qRT-PCR
dsEonuGR1	TAATACGACTCACTATAGGG ATGCCATTTGGTATTGGACAAG	TAATACGACTCACTATAGGG CTAAATTTGATCCATGATTCTTAAAGTTCTTG	RT-PCR
β-actin	AGCGTGGTTACTCTTTCA	GCAACTCGTAGGACTTCT	qRT-PCR

2.3. Genetic Cloning

Based on the previous full-length mRNA sequencing of *E. onukii*, we obtained mRNA (with complete cds) of the EonuGR1 protein, and mRNA sequences were further validated via PCR and sequencing [39].

The PCR products were tested via 1% agarose gel electrophoresis with electrophoresis buffers 1× TAE (Vazyme, Nanjing, China), then DNA fragments of matching length were cut and recovered. Next, the plasmid was purified through FastPure® Plasmid Mini Kit (Vazyme, Nanjing, China) and ligated into the pET-30a vector. The 10 μL of the plasmids were transformed into *Escherichia coli* DH5α, and the transformation conditions were 0 °C for 25 min, 42 °C for 90 s, then 0 °C for 5 min. Next, nonresistant LB solution 100 μL was added, and the plasmids were placed in a 37 °C incubator and shaken for 2 h. The plates were coated and then incubated in a 37 °C incubator for 12 h, and 20 positive cloned monocultures were selected in LB liquid medium containing 100 mg/mL kanamycin after overnight incubation at 37 °C. Then, the bacteriophage was identified by PCR. The PCR system for the identification of bacterial broth was 5 μL of 2× Taq Master Mix, 0.4 μL each of 10 μmol/L forward and reverse primers, 3.2 μL of ddH_2O, and 1 μL of bacterial broth. The reaction conditions for PCR were the same as in Methods 2.2.

2.4. Bioinformatic Techniques

Putative signal peptide was tested via SignalP 3.0 Server (https://services.healthtech.dtu.dk/service.php?SignalP-5.0, accessed on 1 December 2022). Theoretical isoelectric point, calculated molecular weight, and grand average of hydropathicity were detected via ProtParm Tool (https://web.expasy.org/protparam/, accessed on 1 December 2022). Transmembrane domains and protein subcellular localization were forecasted via the

DeepTMHMM (https://dtu.biolib.com/DeepTMHMM, accessed on 1 December 2022) and WoLF PSORT (https://wolfpsort.hgc.jp/, accessed on 1 December 2022), respectively. Secondary and tertiary structures were forecasted via Sopma (https://npsa-prabi.ibcp.fr/cgi-bin/npsa_automat.plpage=npsa_sopma.html, accessed on 1 December 2022) and Swiss-Model (https://swissmodel.expasy.org/interactive, accessed on 1 December 2022), respectively. Protein phosphorylation sites were tested via NetPhos Server (http://www.cbs.dtu.dk/services/NetPhos/, accessed on 1 December 2022). Hydrophilicity or hydrophobicity of EonuGR1 were analyzed via protscale (https://web.expasy.org/protscale/, accessed on 1 December 2022). Nucleotide sequence similarity of related species of EonuGR1 was compared via BLASTN (http://blast.ncbi.nlm.nih.gov, accessed on 1 December 2022) of NCBI, and DNAMAN9.0 was used for amino acid sequence homology analysis of different species. Phylogenetic tree was built by the method of neighbor-joining using MEGA version 11 software, and the bootstrap value of the test was set to 1000 [40].

2.5. Expression Profiles of EonuGR1 in Diverse Tissues

The full-length sequence of *EonuGR1* was obtained via PCR amplification, and based on the results, qPCR-specific primers GR1-qF/GR1-qR. The β-actin (BETA-actin), as an internal reference gene, was used to design the specific primers β-actin-F/β-actin-R to determine the relative expression of *EonuGR1* (Table 1). The reaction system for qPCR was 10 μL of 2 × ChamQ SYBR qPCR Master Mix, each 0.4 μL of 10 μm forward and reverse primers, 0.4 μL of 50× ROX Reference Dye1, 1 μL of template cDNA, 7.8 μL of ddH_2O. The thermal cycling conditions were 95 °C for 30 s, then 40 cycles of 95 °C for 10 s, 60 °C for 30 s, finally, 95 °C for 15 s. During the qRT-PCR, three biological replicates were set up, and the expression profiles of *EonuGR1* in various tissues (antennae, head, thorax, abdomen, and leg) of sex adult *E. onukii* were detected via the $2^{-\Delta\Delta Ct}$ method [41].

2.6. Synthesis of dsRNA

The *EonuGR1* gene fragments were cloned into the pET-30a vector and transformed into *E. coli* DH5α. The amplification reactions were performed at 95 °C for 3 min, then 35 cycles of 95 °C for 15 s, 55 °C for 15 s, then 72 °C for 60 s, followed by incubation at 72 °C for 5 min. The plasmid was fetched and validated by Shenggong Bioengineering (Shanghai, China) Co., Ltd. Sequencing was then used for dsRNA synthesis via a T7 RNAi Transcription Kit (Vazyme, Nanjing, China). Plasmid purification was performed by the magnetic bead method, and then the purified dsRNAs were checked via spectroscopy. Next, dsRNAs were tested by 1% agarose gel electrophoresis to recognize validity.

2.7. Delivery of dsRNA via Foliar Spray and Root Soak

The following steps for dsRNA feeding are illustrated. The prepared RNAi fragment product was thawed at −80 °C and adjusted to a concentration of 1000 ng/μL. Next, 400 μL of dsEonuGR1 were pipetted into 1.5 mL RNase-free microfuge tubes (Thermo Fisher, USA). The roots of a 'Longjing 43' tea seedling were cleaned with sterile water, and the roots were air-dried until there were no droplets. Next, the roots were placed in centrifuge tubes with dsEonuGR1 and treated as root soak. A 'Longjing 43' tea seedling was placed in a centrifuge tube with sterile water, and approximately 400 μL of dsEonuGR1 solution was sprayed directly onto the leaves of tea seedlings and treated as a foliar spray. On the basis of the above treatment, the tea seedlings were enveloped with glass test tubes (30 × 200 mm), and 40 adult *E. onukii* were inserted into each test tube. The glass test tubes were sealed intact with sealing film. The test tubes were placed vertically upside down in the plant incubator, with 25–28 °C, 45–50% rh humidity, 4000 LX light intensity, and 12 h photoperiod. Sample collection time was scheduled at 3, 12, 24, and 48 h after treatment, and 3 replicates of 10 *E. onukii* each were treated and frozen for use in liquid nitrogen. Non-experimentally treated *E. onukii* adults were used as the control group, and the interference efficiency of different treatments on *EonuGR1* was analyzed using qRT-PCR by the same test procedure as in Methods 2.5.

2.8. Y-Tube Olfactometer Assays

In our previous research, olfactory responses of *E. onukii* to 1-phenylethanol, acetophenone, and phenylacetaldehyde were studied [42], and the results showed that the *E. onukii* adults were more attracted to volatiles, including phenylacetaldehyde at a concentration of 10 µL/mL, acetophenone as well as 1-phenylethanol at a concentration of 100 µL/mL. A Y-tube olfactometer was used to determine the behavioral changes of *E. onukii* in response to tea plant volatile compounds after interference with *EonuGR1*. To examine the interference efficiency, *E. onukii* was tested for response to compounds after 3 h and 12 h of *EonuGR1* interference. The Y-tube olfactometer was composed of a 60-mm-long base tube and two 60-mm-long arms at a 90° angle to each other. Both side arms of the Y-tube olfactometer were connected to the taste source bottle, and the airflow was provided by a vacuum pump. The airflow entered the two side arms of the olfactometer through activated charcoal and humidification bottles, and the flow rate into the side arms was controlled at 400 mL/min. Adult *E. onukii* entered the olfactometer from the end of the main arm. Each adult *E. onukii* was individually introduced into the main arm entrance of the Y-tube olfactometer, then, the *E. onukii* were observed for 5 min. If the experimental *E. onukii* entered either arm for more than 3 cm and stayed for at the fewest 1 min, the result was found to be 'choice'. If the experimental *E. onukii* did not make a tangible choice in less than 5 min, the result was found to be 'no choice'. After 15 insects were tested, the odor source position was inverted to prevent location effects. The Y-tube olfactometer was washed using acetone (98%, Macklin) and heated at 100 °C for experimentation again after every 15 *E. onukii* were tested. Thirty *E. onukii* adults were treated with each odor source treatment, and the experiment time was 17:00 h–21:00 h.

2.9. Homology Modelling and Molecular Docking

The main purpose of homology modeling is to predict the structure from its sequence with an accuracy similar to experimental results, thus providing a viable and cost-effective alternative to generate models [43,44]. Molecular docking could provide insight into intermolecular interactions, which is an important tool for predicting the binding type and interaction pattern of biomolecular complexes and providing a useful reference base and theoretical support for further experiments [45,46]. Molecular docking was applied to explore the manner of binding of ligands to *EonuGR1* via AutoDock Vina version 1.1.2 [47]. Next, the docking input files were generated via AutoDock Tools version 1.5.7 [48]. Blind docking was conducted. For Vina docking, the experimental parameters were set according to the default parameters in the manual. The most excellent conformation of the EonuGR1/ligand complex was measured by the lowest calculated binding free energy. Then, the docked models of *EonuGR1* interacting with ligands were built via Discovery Studio version 2021 software and were subjected to visual analysis via PyMOL (http://www.pymol.org/, accessed on 1 December 2022).

2.10. Statistical Analysis of Data

All data were input into an Excel spreadsheet for statistical purposes. The statistical analyses of the number of compounds attracted to *E. onukii* and the *EonuGR1* expression level were conducted using SPSS version 20.0 software. The data were analyzed using LSD and S-N-K tests, and the level of significance was at $p = 0.05$. The descriptive statistics were expressed as the mean value and standard errors of the mean. The indoor entrapment effect of *E. onukii* on compounds was analyzed using the chi-squared test, and the significance threshold was * $p < 0.05$; ** $p < 0.01$. Images were drawn by Origin version 2021 software.

3. Results

3.1. Sequence Prediction Analysis of EonuGR1

The sequence obtained was identified by NCBI as the EonuGR1 sequence (accession number OP999218). The full-length ORF was composed of 1062 nucleotides and encoded 354 amino acid residues. The molecular weight of the EonuGR1 protein was 40.52 kD,

and the PCR-amplified sequences were examined by gel electrophoresis (Figure 1). The prediction of the transmembrane structural domain showed 7 typical transmembrane helix regions between amino acids located at 19–34, 56–74, 109–127, 142–166, 214–235, 243–264, and 324–354 (Figure 2a). There were 26 phosphorylation sites in the EonuGR1 protein, mainly concentrated in serine and threonine (Figure 2b), and it did not contain a signal peptide (Figure 2c). According to glycosylation site prediction, there were 51 glycosylation sites in the EonuGR1 protein, mainly serine and threonine (Figure 2d). The hydrophobic region of the EonuGR1 protein was larger than the hydrophilic region, with an overall average hydrophilic value of 0.565. Combined with the location of the transmembrane region, this value indicates that the transmembrane region of the EonuGR1 protein was hydrophobic (Figure 2e). As shown in Table S1 and Figure 2f, α-helices and irregular coils were the major secondary structural components of the EonuGR1 protein, accounting for 57.22% and 22.66% of the total structure, respectively, while β-strands accounted for only 1.42%. In the tertiary structure prediction, the conserved structural domain of 7tm_7 (positions 1–346) was contained in EonuGR1 protein. There was an intracellular N-terminus and an extracellular C-terminus in EonuGR1 protein.

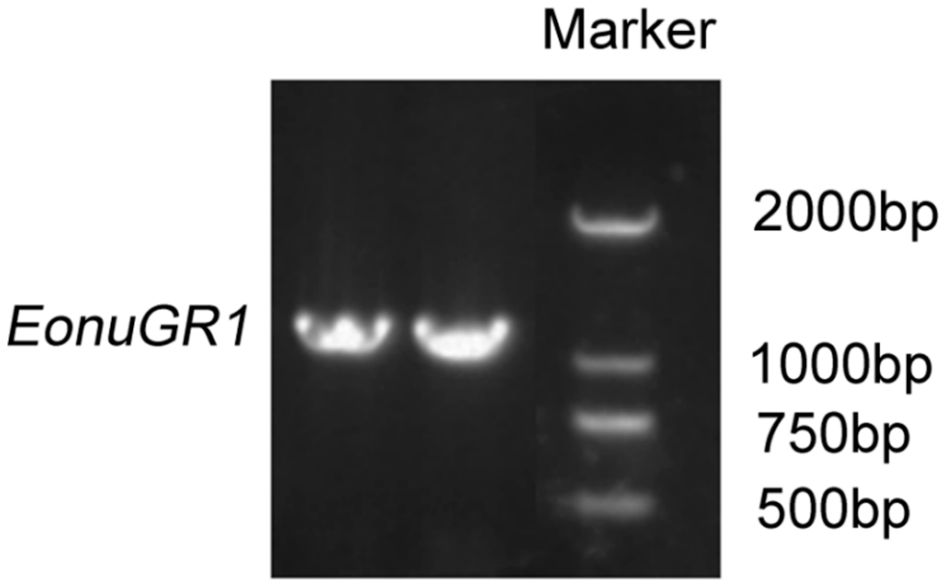

Figure 1. PCR amplification of the *EonuGR1* gene.

3.2. Sequence Alignment and Tissue Expression Profiling

The sequence similarity of *EonuGR1* and other Hemiptera GRs ranged from 15% to 20%. The similarity between *EonuGR1* and *HvitGR1* (KAG8299343.1) was 17.14%, while the similarity of *EonuGR1* to *NvirGR1* (CAH1401484.1) and *AlucGR1* (KAF6207104.1) was 16.19% and 16.67%, respectively. The sequence similarity of *EonuGR1* to *SyanGR22* (AXY87931.1) was low at 15%. In particular, similar sequences converged in the middle and at the end, according to the comparison of *EonuGR1* with other Hemiptera GRs (Figure 3a). The phylogenetic tree showed that *EonuGR1* clustered with GR22 and GR63a of *Apolygus lucorum*, *Aphis gossypii*, *Myzus persicae*, and *Acyrthosiphon pisum*, and it was in a minimal branch alone (Figure 3b). After kinship prediction, tissue expression profiles were determined, and *EonuGR1* was mainly expressed in the abdomen of male and female adults, with expression amounts of 3.01 ± 0.08 and 2.76 ± 0.10, respectively, which were higher than those in other tissues in *E. onukii* (Figure 3c). The expression of *EonuGR1* in the abdomen of male and female adults was 21.5-fold and 23-fold higher than that in the legs, respectively. In addition, the expression of *EonuGR1* in the antennae of male and female adults was comparable and higher than those in the head and thorax, with expression levels of 1.10 ± 0.08 and 1.10 ± 0.35, respectively, which were approximately 2.5-fold and 3.3-fold higher than those in the thorax and abdomen. There was no significant difference between male and

female adults in the same tissue ($p > 0.05$). However, there was a significant difference in expression between diverse tissues of the same sex ($F = 78.303$, $d.f. = 9$, $p < 0.01$).

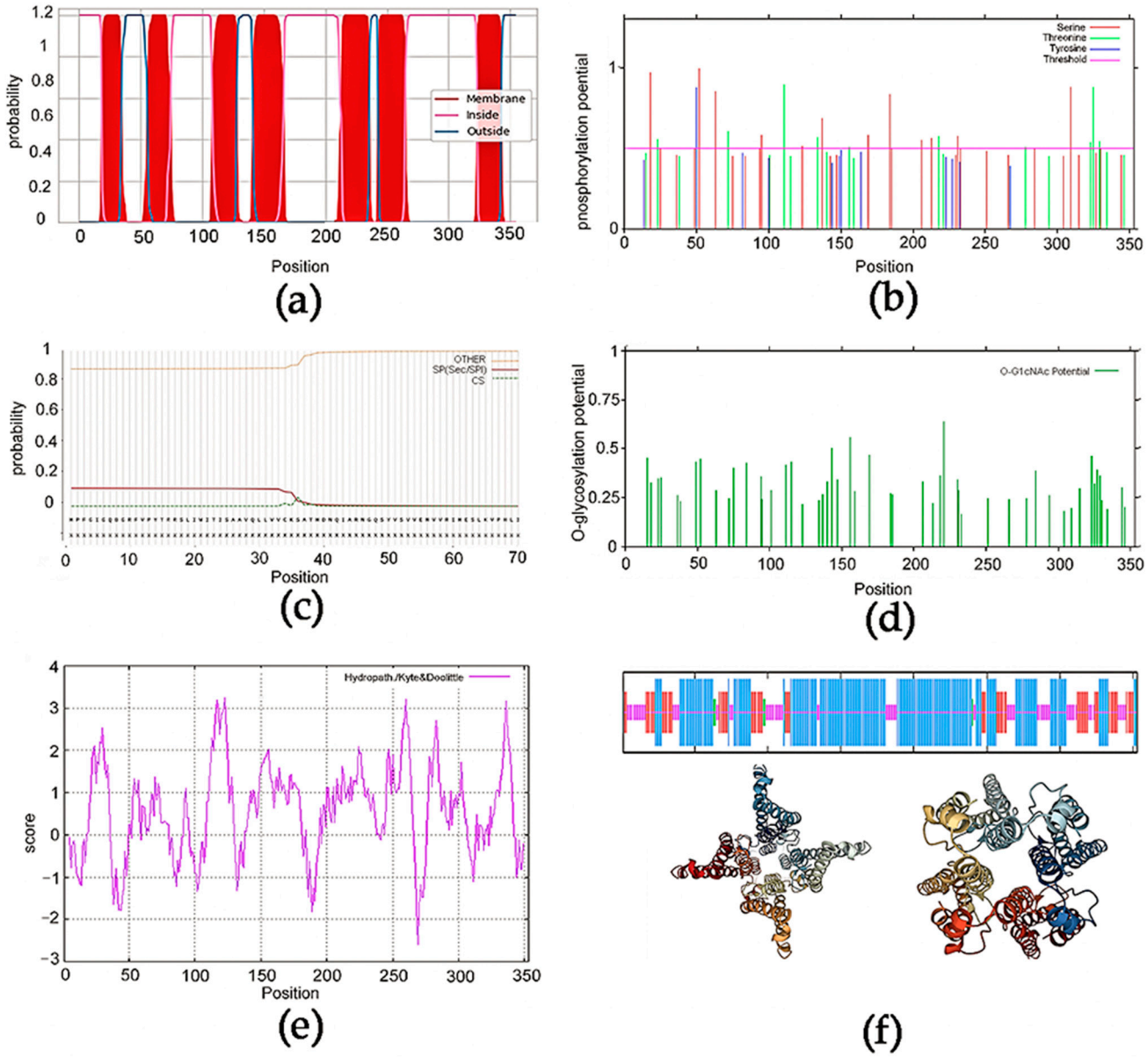

Figure 2. Prediction of EonuGR1 protein in *E. onukii*. (**a**) Transmembrane domain analysis of the EonuGR1 protein. (**b**) Phosphorylation site analysis of the EonuGR1 protein. (**c**) Protein signal peptide analysis of the EonuGR1 protein. (**d**) Glycosylation site analysis of the EonuGR1 protein. (**e**) Hydrophilic analysis of the EonuGR1 protein. (**f**) Secondary and tertiary structure prediction of the EonuGR1 protein.

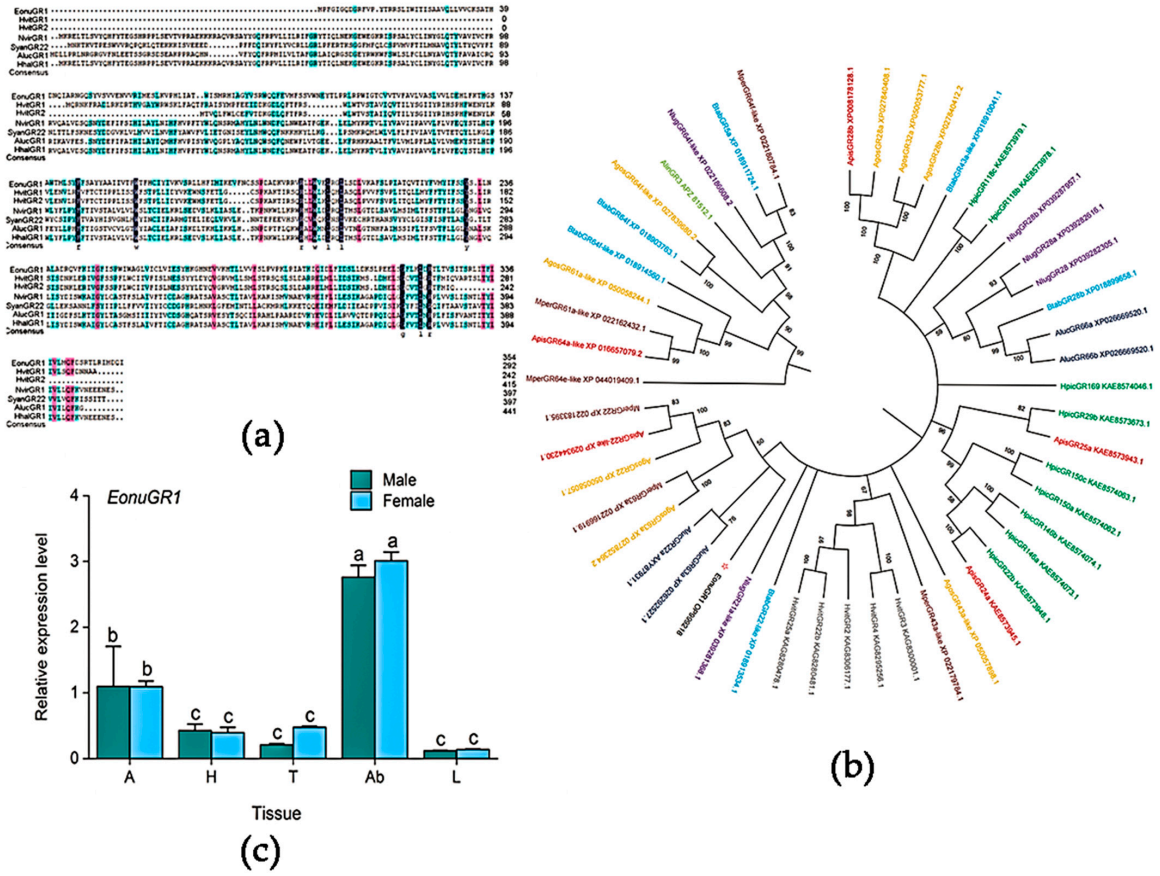

Figure 3. Sequence analysis and tissue expression profile of *EonuGR1*. (**a**) Multiple sequence comparison of *EonuGR1* and GRs of hemipteran insects. (**b**) Phylogenetic tree of *EonuGR1* and GRs of hemipteran insects. (**c**) Expression distribution of *EonuGR1* in different tissues. Note: (**a**) Black regions represent the similarity of 100%, pink regions represent the similarity of more than 75%, blue regions represent the similarity of more than 50%. (**b**) Various insect species are represented by diverse colors in evolutionary tree. Black indicates *Empoasca onukii*; Red indicates *Acyrthosiphon pisum*; Orange indicates *Aphis gossypii*; Blue indicates *Bemisia tabaci*; Green indicates *Halyomorpha picus*; Purple indicates *Nilaparvata lugens*; Navy blue indicates *Apolygus lucorum*; Brown indicates *Myzus persicae*; Olive green indicates *Adelphocoris lineolatus*; Grey indicates *Homalodisca vitripennis*. The number on the branch indicates the confidence value, and the *EonuGR1* is represented by a red star. (**c**): A: antennae; H: head; T: thorax; Ab: abdomen; L: leg. Data are mean ± SE in the figure. Diverse lowercase letters on bars of the same color demonstrate significant differences in the relative expression levels of *EonuGR1* among diverse tissues of male and female adults by LSD and S-N-K ($p < 0.05$).

3.3. In Vitro Synthesis and RNAi Interference Efficiency Analysis

dsEonuGR1 was synthesized in vitro using the T7 RNAi Transcription Kit and verified by 1% gel electrophoresis, which showed a bright single band at approximately 1000 bp, indicating that the sequence length of the synthesized product was in tune with the size of *EonuGR1* (Figure 4a). The concentrations of the products were measured to be above 2500 ng/μL, which was sufficient to interfere with *EonuGR1* and met the criteria to be used in subsequent experiments. The expression of *EonuGR1* decreased significantly after 3 h of *E. onukii* feeding on foliar spray with dsEonuGR1. Its expression was 0.41 ± 0.03, and at 48 h, it was 0.84 ± 0.04. There was a highly significant difference between the expression of the different time treatments on the foliar spray treatment and control ($p < 0.01$). The expression of *EonuGR1* decreased to 0.24 ± 0.01 after 3 h and 0.80 ± 0.06 at 48 h after root soak treatment. There was a significant difference in expression between the disparate time

treatments ($p = 0.03$). The interference efficiency of foliar spray treatment on *EonuGR1* at 3, 12, 24, and 48 h was 59.05%, 54.31%, 23.30%, and 16.43%, respectively, while it was 75.67%, 48.04%, 41.07%, and 19.93% at 4 time points of root soak treatment (Figure 4b).

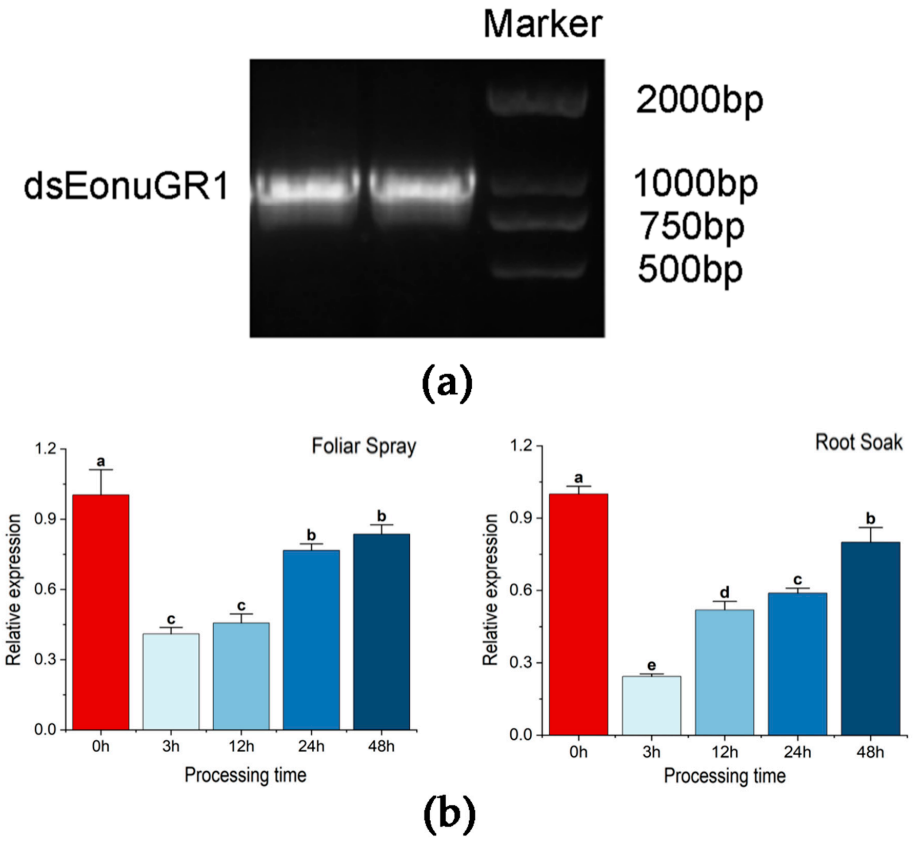

Figure 4. Interference efficiency of feeding dsEonuGR1 to *E. onukii*. (**a**) PCR amplification of dsEonuGR1. (**b**) Interference efficiency of different feeding methods on *EonuGR1*. Note: β-Actin, as a reference gene, was used for the assay of *EonuGR1* expression profiles in disparate tissues. Data are the mean ± SE, and lowercase letters represent significant differences ($p < 0.05$).

3.4. Responses to Compounds after Interferencing with EonuGR1 in E. onukii

The RNAi efficiency showed that the root soak treatment was more stable and superior to foliar spray. Therefore, *E. onukii* interferenced with *EonuGR1* for 3 and 12 h were tested with a Y-type olfactometer. After 3 h, the response rates of *E. onukii* to phenylacetaldehyde at concentrations of 10 μL/mL ($\chi^2 = 18.484$, *d.f.* = 1, $p < 0.01$), 0.1 μL/mL ($\chi^2 = 5.272$, *d.f.* = 1, $p = 0.022$) and 1-phenylethanol at a concentration of 10 μL/mL ($\chi^2 = 0.521$, *d.f.* = 1, $p < 0.01$) were significantly downregulated by 33.33%, 20%, and 30%, respectively (Figure 5a). After *E. onukii* interferencing with *EonuGR1* for 12 h, the response of *E. onukii* to phenylacetaldehyde at concentrations of 10 μL/mL ($\chi^2 = 7.521$, *d.f.* = 1, $p < 0.01$) and 100 μL/mL ($\chi^2 = 0.18$, *d.f.* = 1, $p > 0.05$) and to acetophenone at a concentration of 10 μL/mL ($\chi^2 = 1.636$, *d.f.* = 1, $p > 0.05$) showed a significant decrease in the response of 30%, 30%, and 33.33%, respectively, and a highly significant difference between phenylacetaldehyde at a concentration of 10 μL/mL and the control (Figure 5b).

3.5. Homology Modeling and Molecular Docking

Binding models showed that most of the ligands were bound to the hydrophobic cavity of *EonuGR1*, and were close to the majority of hydrophobic residues near numerous hydrophobic residues. As the docking results showed, the binding energies of 1-phenylethanol, acetophenone, and phenylacetaldehyde with *EonuGR1* were −4.79, −4.81,

and −5.05, respectively. The ligand energies of the three compounds bound to *EonuGR1* were −0.56, −0.53, and −0.53, respectively (Figure 6).

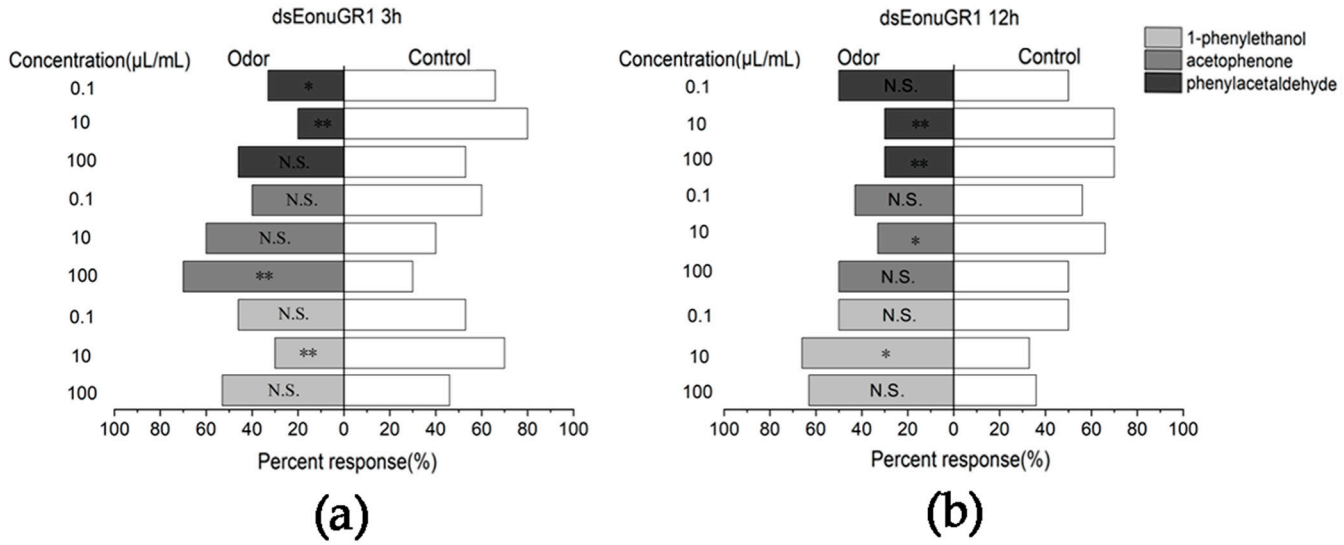

Figure 5. Response rate to compounds after interference with *EonuGR1* by *E. onukii.* (**a**) Response rate of *E. onukii* to compounds after 3 h of interference with *EonuGR1*. (**b**) Response rate of *E. onukii* to compounds after 12 h of interference with *EonuGR1*. Note: Asterisks represent significant differences in a selection test (* $p < 0.05$; ** $p < 0.01$); N.S. represents no significant difference.

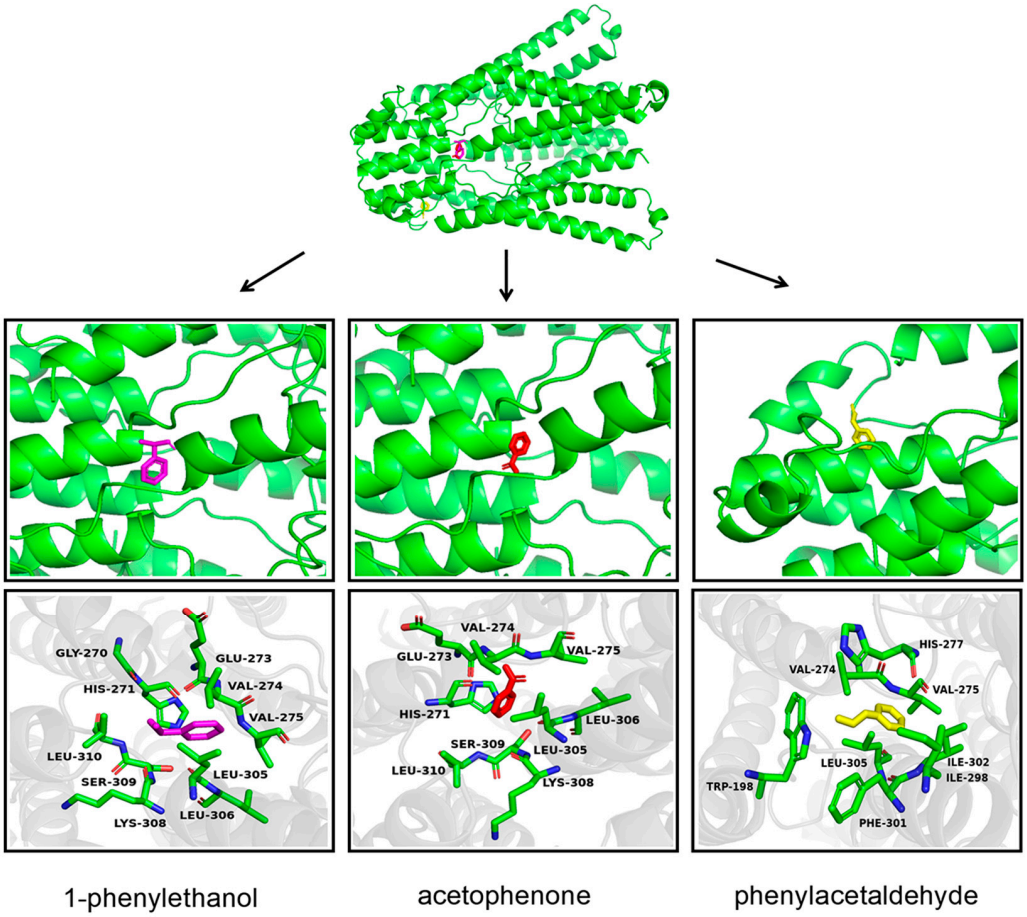

Figure 6. The key residues of the different ligands: 1-phenylethanol, acetophenone, and phenylacetaldehyde that interact with *EonuGR1*.

4. Discussion

Gustation has a pivotal effect on insect survival strategies, and it is therefore essential to explore insect gustatory receptors [12]. In this study, the sequence of *EonuGR1* was obtained by cloning in *E. onukii*, with 7 transmembrane structural domains. There was an intracellular N-terminus and an extracellular C-terminus in EonuGR1 protein, and the present results were similar to those of previous studies [11,24]. The conserved domain 7tm_7 (positions 1–346) was found in *EonuGR1*, classified as a G protein-coupled receptor, a family that includes gustatory and odor receptors. The family is mainly derived from insects, such as *D. melanogaster* and *Anopheles gambiae*, showing a relatively significant sequence divergence and consistent with the ancient origin [49,50]. In our results, the sequence similarity between *EonuGR1* and other hemipteran insect GRs ranged from 15% to 20%, and *EonuGR1* has a relatively high sequence similarity of 17.14% with *HvitGR1*, which is associated with a high degree of GR differentiation [7]. The sequence similarity of lepidopteran insect GRs ranged from 10% to 95% due to the evolution of the GRs from olfactory genes of ancient parents [51,52]. *EonuGR1* clustered with GR22 and GR63a of Lepidoptera insects, such as *A. lucorum*, *A. gossypii*, and *M. persicae*, suggesting that they may belong to the same class of proteins and perform similar functions. GR22 is highly conserved among different species, such as *Tribolium castaneum*, *A. gambiae*, *Aedes aegypti*, and *Bombyx mori*, and it has important functions in insects [49,53,54].

In this study, *EonuGR1* was highly expressed mainly in the abdomen of adult *E. onukii*, followed by high expression in the antennae. GRs were distributed differentially in the thoracic, ventral, and reproductive organs, and it is speculated that these GRs are related to courtship localization [55–57]. Injection of *NlugGR7* into female adult *N. lugens* showed a reduction in ovarian yolkogenic protein in the ovaries, with implications for population reproduction [58]. GR33a functions in the detection of nonvolatile and repulsive chemicals, such as male pheromones, involved in the courtship and reproduction process in *D. melanogaster* [59]. Whether the specific expression of *EonuGR1* in the abdomen is related to its courtship and reproductive behaviors should be further investigated via RNAi. Notably, GRs are distributed widely in gustatory tissues, such as the labellum, upper lip, pharynx, antennae, and mandibular whiskers, and are linked inextricably to many olfactory and gustatory receptors in insect heads [60]. The expression level of *EonuGR1* in antennae is high, which is similar to the expression of *BtabGR1* and *BtabGR2* in *Bemisia tabaci*, and the *Heliothis virescens* GRs are also distributed mainly in the antennae, which is associated with the reams of gustatory receptors in the head [61,62]. DmGR genes exist in abdominal tissues and taste organs, which is similar to our results [63,64].

RNAi has become a crucial technique for gene function exploration and a potential means of pest control [65–67]. The changes in *EonuGR1* RNAi efficiency via foliar spray decreased by 31.01%, mainly from 12 to 24 h. Root soak treatments decreased by 31.01% and 21.14% from 3 to 12 h and 24 to 48 h, respectively. Decreases in RNAi efficiency were mainly concentrated in the early stage, with gene expression being lowest at 3 h, and RNAi was significantly more effective and stable via root soak treatment than via foliar spray treatment. Delivering dsRNA by root absorption or injection into plant vessels could deliver dsRNA to phytophagous insects that naturally acquire dsRNA through sucking or chewing [68]. The roots of rice plants were immersed in a solution containing dsRNA targeting carboxylesterase and a cytochrome P450 (Cyp18A1) from *N. lugens*. When the *N. lugens* nymphs fed on treated plants, the target genes were knocked down, thus leading to high mortality in insects [69]. The dsRNAs were absorbed through root soaking into the plant vascular bundle and remained there for a long time, possibly increasing insect mortality [70]. Likewise, *Ostrinia furnacalis* was observed to have a high mortality rate when maize seedlings were irrigated with dsRNA of Kunitz-type trypsin inhibitors [71]. The processing of dsRNAs into siRNAs via endogenous plant RNAi pathways also affects their efficiency [69,72]. Our experiments verified that root soak treatment and interference for 3 h were the best method and experimental time for interference with *E. onukii* genes, respectively.

Insect GRs can recognize a wide range of substances, including sugar substances such as fructose [18,73,74], sucrose [75], glucose [76], and maltotriose [20], as well as bitter substances including strychnine [30], nicotine [36], caffeine [77] and saponin [78]. In particular, GRs also have recognition functions for individual volatiles. For example, *TchiGR43a* tunes both fructose and inositol in *Trichogrammachilonis* [79]. GR61a and GR5a can function in the detection of amino acids in *D. melanogaster* [80,81]. *PxylGR34* is a relevant receptor for the detection of brassinolide and 24-epibrassinolide in *P. xylostella* [37]. Previous studies showed that 63%, 70%, and 67% of *E. onukii* adults responded to phenylacetaldehyde at concentrations of 0.1, 10, and 100 μL/mL and were more attracted to phenylacetaldehyde at concentrations of 10 and 100 μL/mL [42]. After interference with *EonuGR1* for 3 h, the responses to acetophenone decreased insignificantly, with no significant differences from the controls, and some decrease for 1-phenylethanol at 10 μL/mL, but no significant differences at other concentrations in *E. onukii*. However, the responses of *E. onukii* to phenylacetaldehyde at concentrations of 0.1 and 10 μL/mL were significantly downregulated. At 12 h, the response rate to acetophenone and 1-phenylethanol was less variable and not significantly different from the control in *E. onukii*. However, the responses to phenylacetaldehyde at 10 and 100 μL/mL decreased significantly. The injection of dsPxutGR1 into the body strongly reduces ovulatory behavior in response to synephrine in *Papilio xuthus*, thereby affecting host localization [36]. The behavioral selection probability for phenylacetaldehyde was reduced after interference with *EonuGR1*, and considering this information and its high expression in the abdomen of adults, we speculated that *EonuGR1* may participate in oviposition localization through its involvement in phenylacetaldehyde recognition in *E. onukii*. Olfaction sensing allows organisms to recognize volatile cues in insects and gustatory receptors may be involved in their localization through olfactory host recognition [82].

Insect gustatory and olfactory stimulus interactions play a role in the perception of host localization [81]. In addition, the docking results showed a binding energy value of -5.05 between *EonuGR1* and phenylacetaldehyde, which was higher than its binding ability with 1-phenylethanol (−4.79) and acetophenone (−4.81), thus predicting a stronger recognition ability of *EonuGR1* for phenylacetaldehyde. The interactions of key residues were predicted, such as VAL, TRP, ILE, and LEU, with hydrophobic residues, especially TRP-198, suggesting they may function in the binding of *EonuGR1* to phenylacetaldehyde. Based on the functions of insect GRs in host localization, GR-targeted pest control strategies have been proposed. For example, silencing *PxylGR34* via RNAi caused aversive behavior of adult *P. xylostella* to oleoresinolide, thus reducing pest damage to the host crop [37]. In our study, we clarified the biological information and expression profile of *EonuGR1* and made an attempt for the function of *EonuGR1* in recognizing tea tree volatiles, which provides a reference for elucidating the molecular mechanism of GRs in *E. onukii*.

Supplementary Materials: The following supporting information can be downloaded at: https://www.mdpi.com/article/10.3390/agronomy13092221/s1, Table S1 in the article have been added to the supplementary material. Table S1: Amino acid composition of EonuGR1 protein.

Author Contributions: All authors conceived the ideas and designed methodology; contributed to the manuscripts and final submission. X.L., Y.Z. (Yunhe Zhao) and Y.Z. (Yu Zhang) conceived the research and performed the experiments. Y.C., X.Z. and M.J. analyzed and summarized the experimental data. R.Z. performed the writing—original draft preparation. Z.Z. secured funding and critically revised the manuscript, and X.X. validated the manuscript. All authors have read and agreed to the published version of the manuscript.

Funding: We acknowledge financial support from National Natural Science Foundation of China (32102303), Natural Science Foundation of Shandong Province (ZR2020MC122; ZR2020QC132; ZR2020QC055), Development Program of Shandong Province (2022LZGCQY020), Project of Laoshan District Tea Innovation Group (LSCG2022000017), Key Research and Project for Technological Innovation and Development of Tai'an (2021NS082), Project for Special Commissioners in Agricultural Science and Technology of Tai'an (2021TPY021).

Data Availability Statement: The raw data supporting the conclusions of this article will be made available by the authors, without undue reservation.

Acknowledgments: We thank the reviewers and editors for their constructive comments on earlier versions of the manuscript.

Conflicts of Interest: The authors declare no conflict of interest.

References

1. da Silva Pinto, M. Tea: A New Perspective on Health Benefits. *Food Res. Int.* **2013**, *53*, 558–567. [CrossRef]
2. Jin, S.; Chen, Z.M.; Backus, E.A.; Sun, X.L.; Xiao, B. Characterization of EPG Waveforms for the Tea Green Leafhopper, *Empoasca vitis* Göthe (Hemiptera: Cicadellidae), on Tea Plants and Their Correlation with Stylet Activities. *J. Insect Physiol.* **2012**, *58*, 1235–1244. [CrossRef] [PubMed]
3. Yin, P.; Dai, J.X.; Guo, G.Y.; Wang, Z.H.; Liu, W.; Liu, X.; Chen, H.P. Residue Pattern of Chlorpyrifos and Its Metabolite in Tea from Cultivation to Consumption. *J. Sci. Food Agric.* **2021**, *101*, 4134–4141. [CrossRef]
4. Lin, L.; Cheng, S.; Li, J.; Huang, M.; Zhu, D. Effects of Tea Tree Oils on Removing Pesticide Residue in Cowpea. *Nongye Gongcheng Xuebao/Trans. Chin. Soc. Agric. Eng.* **2013**, *29*, 273–278.
5. Morinaga, S.; Nagata, K.; Ihara, S.; Yumita, T.; Niimura, Y.; Sato, K.; Touhara, K. Structural Model for Ligand Binding and Channel Opening of an Insect Gustatory Receptor. *J. Biol. Chem.* **2022**, *298*, 102573. [CrossRef]
6. Liu, H.; Sun, X.; Shi, Z.; An, X.; Khashaveh, A.; Li, Y.; Gu, S.; Zhang, Y. Identification and Functional Analysis of Odorant-Binding Proteins Provide New Control Strategies for *Apolygus lucorum*. *Int. J. Biol. Macromol.* **2023**, *224*, 1129–1141. [CrossRef]
7. Agnihotri, A.R.; Roy, A.A.; Joshi, R.S. Gustatory Receptors in Lepidoptera: Chemosensation and Beyond. *Insect Mol. Biol.* **2016**, *25*, 519–529. [CrossRef] [PubMed]
8. Clyne, P.J.; Warr, C.G.; Carlson, J.R. Candidate Taste Receptors in *Drosophila*. *Science* **2000**, *287*, 1830–1834. [CrossRef]
9. Scott, K.; Brady, R.J.; Cravchik, A.; Morozov, P.; Rzhetsky, A.; Zuker, C.; Axel, R. A Chemosensory Gene Family Encoding Candidate Gustatory and Olfactory Receptors in *Drosophila*. *Cell* **2001**, *104*, 661–673. [CrossRef]
10. Scott, K. Gustatory Processing in *Drosophila melanogaster*. *Annu. Rev. Entomol.* **2018**, *63*, 15–30. [CrossRef]
11. Zhang, H.J.; Anderson, A.R.; Trowell, S.C.; Luo, A.R.; Xiang, Z.H.; Xia, Q.Y. Topological and Functional Characterization of an Insect Gustatory Receptor. *PLoS ONE* **2011**, *6*, e24111. [CrossRef]
12. Xu, W.; Anderson, A. Carbon Dioxide Receptor Genes in Cotton Bollworm *Helicoverpa armigera*. *Naturwissenschaften* **2015**, *102*, 11. [CrossRef] [PubMed]
13. Wang, G.Y.; Zhu, J.L.; Zhou, W.W.; Liu, S.; Khairul, Q.M.; Ansari, N.A.; Zhu, Z.R. Identification and Expression Analysis of Putative Chemoreception Genes from *Cyrtorhinus lividipennis* (Hemiptera: Miridae) Antennal Transcriptome. *Sci. Rep.* **2018**, *8*, 12981. [CrossRef] [PubMed]
14. Song, Y.Q.; Dong, J.F.; Chen, Q.X.; Hu, Z.J.; Sun, H.Z. Analysis of the Antennal Transcriptome and Chemoreception-Related Genes of the Bean Bug, *Riptortus pedestris* (Hemiptera: Alydidae). *Acta Entomol. Sin.* **2017**, *60*, 1120–1128. (In Chinese) [CrossRef]
15. He, P.; Engsontia, P.; Chen, G.L.; Yin, Q.; Wang, J.; Lu, X.; Zhang, Y.N.; Li, Z.Q.; He, M. Molecular Characterization and Evolution of a Chemosensory Receptor Gene Family in Three Notorious Rice Planthoppers, *Nilaparvata lugens*, *Sogatella furcifera* and *Laodelphax striatellus*, Based on Genome and Transcriptome Analyses. *Pest Manag. Sci.* **2018**, *15*, 2156–2167. [CrossRef]
16. Kang, K.; Yang, P.; Chen, L.E.; Pang, R.; Yu, L.J.; Zhou, W.W.; Zhu, Z.R.; Zhang, W.Q. Identification of Putative Fecundity-Related Gustatory Receptor Genes in the Brown Planthopper *Nilaparvata lugens*. *BMC Genom.* **2018**, *19*, 970. [CrossRef]
17. Robertson, H.M.; Gadau, J.; Wanner, K.W. The Insect Chemoreceptor Superfamily of the Parasitoid Jewel Wasp *Nasonia vitripennis*. *Insect Mol. Biol.* **2010**, *19*, 121–136. [CrossRef]
18. Ai, D.; Dong, C.; Yang, B.; Yu, C.; Wang, G. A Fructose Receptor Gene Influences Development and Feed Intake in *Helicoverpa armigera*. *Insect Sci.* **2022**, *29*, 993–1005. [CrossRef]
19. Wu, Z.; Tong, N.; Li, Y.; Guo, J.; Lu, M.; Liu, X. Foreleg Transcriptomic Analysis of the Chemosensory Gene Families in *Plagiodera versicolora* (Coleoptera: Chryso, melidae). *Insects* **2022**, *13*, 763. [CrossRef]
20. Dahanukar, A.; Lei, Y.T.; Kwon, J.Y.; Carlson, J.R. Two Gr Genes Underlie Sugar Reception in *Drosophila*. *Neuron* **2007**, *56*, 503–516. [CrossRef]
21. Jiao, Y.C.; Moon, S.J.; Montell, C.A. Drosophila Gustatory Receptor Required for the Responses to Sucrose, Glucose, and Maltose Identified by Mrna Tagging. *Proc. Natl. Acad. Sci. USA* **2007**, *104*, 14110–14115. [CrossRef] [PubMed]
22. Miyamoto, T.; Slone, J.; Song, X.; Amrein, H. A Fructose Receptor Functions as a Nutrient Sensor in the *Drosophila* Brain. *Cell* **2012**, *151*, 1113–1125. [CrossRef] [PubMed]
23. Jones, W.D.; Cayirlioglu, P.; Kadow, I.G.; Vosshall, L.B. Two Chemosensory Receptors Together Mediate Carbon Dioxide Detection in *Drosophila*. *Nature* **2007**, *445*, 86–90. [CrossRef]
24. Xu, W.; Zhang, H.J.; Anderson, A. A Sugar Gustatory Receptor Identified from The Foregut of Cotton Bollworm *Helicoverpa armigera*. *J. Chem. Ecol.* **2012**, *38*, 1513–1520. [CrossRef]
25. Montell, C. A Taste of the *Drosophila* Gustatory Receptors. *Curr. Opin. Neurobiol.* **2009**, *19*, 345–353. [CrossRef] [PubMed]
26. Fujii, S.; Yavuz, A.; Slone, J.; Jagge, C.; Song, X.; Amrein, H. *Drosophila* Sugar Receptors in Sweet Taste Perception, Olfaction, and Internal Nutrient Sensing. *Curr. Biol.* **2015**, *25*, 621–627. [CrossRef]

27. Dweck, H.K.M.; Carlson, J.R. Molecular Logic and Evolution of Bitter Taste in *Drosophila*. *Curr. Biol.* **2020**, *30*, 17–30. [CrossRef]
28. Moon, S.J.; Lee, Y.; Jiao, Y.; Montell, C. A Drosophila Gustatory Receptor Essential for Aversive Taste and Inhibiting Male-To-Male Courtship. *Curr. Biol.* **2009**, *19*, 1623–1627. [CrossRef]
29. Lee, Y.; Moon, S.J.; Wang, Y.; Montell, C. A Drosophila Gustatory Receptor Required for Strychnine Sensation. *Chem. Senses* **2015**, *40*, 525–533. [CrossRef]
30. Poudel, S.; Kim, Y.; Gwak, J.S.; Jeong, S.; Lee, Y. Gustatory Receptor 22e Is Essential for Sensing Chloroquine and Strychnine in *Drosophila* melanogaster. *Insect Biochem. Mol. Biol.* **2017**, *88*, 30–36. [CrossRef]
31. Liu, J.B.; Wu, H.; Yi, J.Q.; Zhang, G.R. Two Gustatory Receptors Are Necessary for Sensing Sucrose in an Egg Parasitoid, *Trichogramma chilonis*. *Chemoecology* **2020**, *30*, 103–115. [CrossRef]
32. Liu, N.Y.; Xu, W.; Papanicolaou, A.; Dong, S.L.; Anderson, A. Identification and Characterization of Three Chemosensory Receptor Families in the Cotton Bollworm *Helicoverpa armigera*. *BMC Genom.* **2014**, *15*, 597. [CrossRef] [PubMed]
33. Liu, Z.; Wang, X.; Lei, C.; Zhu, F. Sensory Genes Identification with Head Transcriptome of the Migratory Armyworm, Mythimna separata. *Sci. Rep.* **2017**, *7*, 46033. [CrossRef] [PubMed]
34. Zhang, J.; Wang, B.; Dong, S.; Cao, D.; Dong, J.; Walker, W.B.; Liu, Y.; Wang, G. Antennal Transcriptome Analysis and Comparison of Chemosensory Gene Families in Two Closely Related Noctuidae Moths, *Helicoverpa armigera* and *H. assulta*. *PLoS ONE* **2015**, *10*, e0117054. [CrossRef]
35. Shim, J.; Lee, Y.; Jeong, Y.T.; Kim, Y.; Lee, M.G.; Montell, C.; Moon, S.J. The Full Repertoire of *Drosophila* Gustatory Receptors for Detecting an Aversive Compound. *Nat. Commun.* **2015**, *6*, 8867. [CrossRef]
36. Ozaki, K.; Ryuda, M.; Yamada, A.; Utoguchi, A.; Ishimoto, H.; Calas, D.; Marion-Poll, F.; Tanimura, T.; Yoshikawa, H. A Gustatory Receptor Involved in Host Plant Recognition for Oviposition of a Swallowtail Butterfly. *Nat. Commun.* **2011**, *2*, 542. [CrossRef]
37. Yang, K.; Gong, X.L.; Li, G.C.; Huang, L.Q.; Ning, C.; Wang, C.Z. A Gustatory Receptor Tuned to the Steroid Plant Hormone Brassinolide in *Plutella xylostella* (Lepidoptera: Plutellidae). *eLife* **2020**, *9*, e64114. [CrossRef]
38. Yang, J.; Guo, H.; Jiang, N.J.; Tang, R.; Li, G.C.; Huang, L.Q.; van Loon, J.J.A.; Wang, C.Z. Identification of a Gustatory Receptor Tuned to Sinigrin in The Cabbage Butterfly Pieris rapae. *PLoS Genet.* **2021**, *17*, e1009527. [CrossRef]
39. Zhang, X.Z. Identification and Expression Analysis of Olfactory ReceptorGenes in *Empoasca onukii* Matsuda. Master's Thesis, Shandong Agricultural University, Tai'an, China, 2022. (In Chinese).
40. Kumar, S.; Stecher, G.; Li, M.; Knyaz, C.; Tamura, K. MEGA X: Molecular Evolutionary Genetics Analysis across Computing Platforms. *Mol. Biol. Evol.* **2018**, *35*, 1547–1549. [CrossRef]
41. Livak, K.J.; Schmittgen, T.D. Analysis of Relative Gene Expression Data Using Real-Time Quantitative Pcr and the $2^{-\Delta\Delta t}$ Method. *Methods* **2001**, *25*, 402–408. [CrossRef]
42. Zhang, R.R.; Lun, X.Y.; Zhang, Y.; Zhao, Y.H.; Xu, X.X.; Zhang, Z.Q. Characterization of Ionotropic Receptor Gene *EonuIR25a* in the Tea Green Leafhopper, *Empoasca onukii* Matsuda. *Plants* **2023**, *12*, 2034. [CrossRef]
43. Valanciute, A.; Nygaard, L.; Zschach, H.; Maglegaard, J.M.; Lindorff-Larsen, K.; Stein, A. Accurate Protein Stability Predictions from Homology Models. *Comput. Struct. Biotechnol. J.* **2022**, *21*, 66–73. [CrossRef] [PubMed]
44. Quan, W.; Wang, Y.; Chen, Y.H.; Shao, Q.; Gong, Y.Z.; Hu, J.W.; Liu, W.H.; Wu, Z.J.; Wang, J.; Ma, S.B.; et al. Screening of Rosmarinic Acid from Salvia Miltiorrhizae Acting on the Novel Target Trpc1 Based on the 'Homology Modelling-Virtual Screening-Molecular Docking-Affinity Assay-Activity Evaluation' Method. *Pharm. Biol.* **2023**, *61*, 155–164. [CrossRef] [PubMed]
45. Fan, J.; Fu, A.; Zhang, L. Progress in Molecular Docking. *Quant. Biol.* **2019**, *7*, 83–89. [CrossRef]
46. Kaur, T.; Madgulkar, A.; Bhalekar, M.; Asgaonkar, K. Molecular Docking in Formulation and Development. *Curr. Drug. Discov. Technol.* **2019**, *16*, 30–39. [CrossRef]
47. Trott, O.; Olson, A.J. Autodock Vina: Improving the Speed and Accuracy of Docking with a New Scoring Function, Efficient Optimization, and Multithreading. *J. Comput. Chem.* **2010**, *31*, 455–461. [CrossRef]
48. Morris, G.M.; Huey, R.; Lindstrom, W.; Sanner, M.F.; Belew, R.K.; Goodsell, D.S.; Olson, A.J. Autodock4 and Autodocktools4: Automated Docking with Selective Receptor Flexibility. *J. Comput. Chem.* **2009**, *30*, 2785–2791. [CrossRef]
49. Hill, C.A.; Fox, A.N.; Pitts, R.J.; Kent, L.B.; Tan, P.L.; Chrystal, M.A.; Cravchik, A.; Collins, F.H.; Robertson, H.M.; Zwiebel, L.J. G Protein-Coupled Receptors in Anopheles gambiae. *Science* **2002**, *298*, 176–178. [CrossRef]
50. Robertson, H.M.; Warr, C.G.; Carlson, J.R. Molecular Evolution of the Insect Chemoreceptor Gene Superfamily in *Drosophila melanogaster*. *Proc. Natl. Acad. Sci. USA* **2003**, *100*, 14537–14542. [CrossRef]
51. Engsontia, P.; Sangket, U.; Chotigeat, W.; Satasook, C. Molecular Evolution of the Odorant and Gustatory Receptor Genes in Lepidopteran Insects Implications for Their Adaptation and Speciation. *J. Mol. Evol.* **2014**, *79*, 21–39. [CrossRef]
52. Hallem, E.A.; Dahanukar, A.; Carlson, J.R. Insect odor and taste receptors. *Annu. Rev. Entomol.* **2006**, *51*, 113–135. [CrossRef] [PubMed]
53. Kent, L.B.; Walden, K.K.O.; Robertson, H.I.M. The Cr Family Ofcandidate Gustatory and Olfactory Receptors in the Yellow-Fevermosquito *Aedes aegypti*. *Chem. Senses* **2008**, *33*, 79–93. [CrossRef] [PubMed]
54. Wanner, K.W.; Robertson, H.M. The Gustatory Receptor Family in the Silkworm Moth Bombyx mori Is Characterized by a Large Expansion of a Single Lineage of Putative Bitter Receptors. *Insect Mol. Biol.* **2008**, *17*, 621–629. [CrossRef]
55. Ahmed, T.; Zhang, T.; Wang, Z.; He, K.; Bai, S. Gene Set of Chemosensory Receptors in the Polyembryonic Endoparasitoid Macrocentrus cingulum. *Sci. Rep.* **2016**, *6*, 24078. [CrossRef] [PubMed]

56. Yi, J.K.; Yang, S.; Wang, S.; Wang, J.; Zhang, X.X.; Liu, Y.; Xi, J.H. Identification of Candidate Chemosensory Receptors in The Antennal Transcriptome of the Large Black Chafer *Holotrichia parallela* Motschulsky (Coleoptera: Scarabaeidae). *Comp. Biochem. Physiol. Part D Genom. Proteom.* **2018**, *28*, 63–71. [CrossRef]
57. Sun, L.; Zhang, Y.N.; Qian, J.L.; Kang, K.; Zhang, X.Q.; Deng, J.D.; Tang, Y.P.; Chen, C.; Hansen, L.; Xu, T.; et al. Identification and Expression Patterns of *Anoplophora chinensis* (Forster) Chemosensory Receptor Genes from the Antennal Transcriptome. *Front. Physiol.* **2018**, *9*, 90. [CrossRef]
58. Ojha, A.; Zhang, W. Characterization of Gustatory Receptor 7 in the Brown Planthopper Reveals Functional Versatility. *Insect Biochem. Mol. Biol.* **2021**, *132*, 103567. [CrossRef]
59. Hu, Y.; Han, Y.; Shao, Y.; Wang, X.; Ma, Y.; Ling, E.; Xue, L. Gr33a Modulates *Drosophila* Male Courtship Preference. *Sci. Rep.* **2015**, *5*, 7777. [CrossRef]
60. Robertson, H.M.; Wanner, K.W. The Chemoreceptor Superfamily in the Honey Bee, *Apis mellifera*: Expansion of the Odorant, but Not Gustatory, Receptor Family. *Genome Res.* **2006**, *16*, 1395–1403. [CrossRef]
61. Krieger, J.; Raming, K.; Dewer, Y.M.; Bette, S.; Conzelmann, S.; Breer, H. A Divergent Gene Family Encoding Candidate Olfactory Receptors of the Moth *Heliothis virescens*. *Eur. J. Neurosci.* **2002**, *16*, 619–628. [CrossRef]
62. Qu, C.; Wang, R.; Li, F.Q.; Luo, C. Cloning and Expression Profiling of Gustatory Receptor Genes *BtabGR1* and *BtabGR2* in *Bemisia tabaci*. *Sci. Agric. Sin.* **2022**, *55*, 2552–2561. (In Chinese) [CrossRef]
63. Thorne, N.; Amrein, H. Atypical Expression of Drosophila Gustatory Receptor Genes in Sensory and Central Neurons. *J. Comp. Neurol.* **2008**, *506*, 548–568. [CrossRef] [PubMed]
64. Park, J.H.; Kwon, J.Y. A Systematic Analysis of Drosophila Gustatory Receptor Gene Expression in Abdominal Neurons Which Project to the Central Nervous System. *Mol. Cells* **2011**, *32*, 375–381. [CrossRef] [PubMed]
65. Vogel, E.; Santos, D.; Mingels, L.; Verdonckt, T.W.; Broeck, J.V. RNA Interference in Insects: Protecting Beneficials and Controlling Pests. *Front. Physiol.* **2019**, *9*, 1912. [CrossRef] [PubMed]
66. Gordon, K.; Waterhouse, P. RNAi for Insect-proof Plants. *Nat. Biotechnol.* **2007**, *25*, 1231–1232. [CrossRef]
67. Chen, S.; Luo, X.; Nanda, S.; Yang, C.; Li, Z.; Zhang, Y.; Zhou, X.; Pan, H. RNAi-Based Biopesticides Against 28-Spotted Ladybeetle *Henosepilachna vigintioctopunctata* Does Not Harm the Insect Predator Propylea Japonica. *J. Agric. Food Chem.* **2023**, *71*, 3373–3384. [CrossRef]
68. Andrade, C.E.; Hunter, W.B. RNA Interference -Natural Gene-Based Technology for Highly Specific Pest Control (HiSPeC). *RNA Interf.* **2016**, *1*, 391–409. [CrossRef]
69. Joga, M.R.; Zotti, M.J.; Smagghe, G.; Christiaens, O. RNAi Efficiency, Systemic Properties, and Novel Delivery Methods for Pest Insect Control: What We Know So Far. *Front. Physiol.* **2016**, *7*, 553. [CrossRef]
70. Li, H.; Guan, R.; Guo, H.; Miao, X. New Insights into an RNAi Approach for Plant Defence against Piercing-Sucking and Stem-Borer Insect Pests. *Plant. Cell Environ.* **2015**, *38*, 2277–2285. [CrossRef]
71. Li, H.; Khajuria, C.; Rangasamy, M.; Gandra, P.; Fitter, M.; Geng, C.; Woosely, A.; Hasler, J.; Schulenberg, G.; Worden, S.; et al. Long dsRNA but Not siRNA Initiates RNAi in Western Corn Rootworm Larvae and Adults. *J. Appl. Entomol.* **2015**, *139*, 432–445. [CrossRef]
72. Zhang, J.; Khan, S.A.; Hasse, C.; Ruf, S.; Heckel, D.G.; Bock, R. Full Crop Protection from an Insect Pest by Expression of Long Double-Stranded Rnas in Plastids. *Science* **2015**, *347*, 991–994. [CrossRef]
73. Liu, X.L.; Yan, Q.; Yang, Y.L.; Hou, W.; Miao, C.L.; Peng, Y.C.; Dong, S.L. A Gustatory Receptor Gr8 Tunes Specifically to D-Fructose in the Common Cutworm *Spodoptera litura*. *Insects* **2019**, *10*, 272. [CrossRef] [PubMed]
74. Liu, X.L.; Sun, S.J.; Hou, W.; Zhang, J.; Yan, Q.; Dong, S.L. Functional Characterization of Two Spliced Variants of Fructose Gustatory Receptor in the Diamondback Moth, *Plutella xylostella*. *Pestic. Biochem. Physiol.* **2020**, *164*, 7–13. [CrossRef]
75. Jung, J.W.; Park, K.W.; Ahn, Y.J.; Kwon, H.W. Functional Characterization of Sugar Receptors in the Western Honeybee, *Apis mellifera*. *J. Asia Pac. Entomol.* **2015**, *18*, 19–26. [CrossRef]
76. Mang, D.; Mayu, K.; Toyama, T.; Yamagishi, T.; Sato, R. BmGR4 Responds to Sucrose and Glucose and Expresses in Tachykinin-Related Peptide-Secreting Enteroendocrine Cells. *Insect Biochem. Mol. Biol.* **2022**, *150*, 103858. [CrossRef] [PubMed]
77. Poudel, S.; Kim, Y.; Kim, Y.T.; Lee, Y. Gustatory Receptors Required for Sensing Umbelliferone in *Drosophila melanogaster*. *Insect Biochem. Mol. Biol.* **2015**, *66*, 110–118. [CrossRef] [PubMed]
78. Sang, J.; Rimal, S.; Lee, Y. Gustatory Receptor 28b Is Necessary for Avoiding Saponin in *Drosophila melanogaster*. *EMBO Rep.* **2019**, *20*, e47328. [CrossRef]
79. Liu, J.; Wu, H.; Yi, J.; Jiang, D.; Zhang, G. Identification and Functional Characterization of D-Fructose Receptor in an Egg Parasitoid, *Trichogramma chilonis*. *PLoS ONE* **2019**, *14*, e0217493. [CrossRef]
80. Aryal, B.; Dhakal, S.; Shrestha, B.; Lee, Y. Molecular and Neuronal Mechanisms for Amino Acid Taste Perception in the *Drosophila labellum*. *Curr. Biol.* **2022**, *32*, 1376–1386.e4. [CrossRef]
81. Shrestha, B.; Lee, Y. Mechanisms of Carboxylic Acid Attraction in *Drosophila melanogaster*. *Mol. Cells* **2021**, *44*, 900–910. [CrossRef]
82. Sánchez-Gracia, A.; Vieira, F.G.; Rozas, J. Molecular Evolution of the Major Chemosensory Gene Families in Insects. *Heredity* **2009**, *103*, 208–216. [CrossRef] [PubMed]

Disclaimer/Publisher's Note: The statements, opinions and data contained in all publications are solely those of the individual author(s) and contributor(s) and not of MDPI and/or the editor(s). MDPI and/or the editor(s) disclaim responsibility for any injury to people or property resulting from any ideas, methods, instructions or products referred to in the content.